An Augmented Finite Volume Formulation for Simulating TDEM Responses From Highly Conductive Plate-Like Targets

D. C. Cowan, L. J. Heagy and D. W. Oldenburg
University of British Columbia Geophysical Inversion Facility, ubcgif@eoas.ubc.ca

SUMMARY

Inductive source time-domain electromagnetic (TDEM) methods are frequently used to image ore-bearing mineralizations that present as thin and highly conductive (>1000 S/m). The need to properly characterize inductive responses from thin, highly conductive targets in geologically complex areas has promoted significant interest in developing improved numerical algorithms. Here, we present an augmented mimetic finite volume formulation that accurately models the physics while limiting the computational resources required. We accomplish this by defining the electrical properties of plate-like structures as conductances that live on voxel faces. The formulation is implemented using the SimPEG framework. The formulation shows excellent agreement when validated against the semi-analytic 1D solution for a thin horizontal layer within a halfspace. Additionally, the formulation is capable of simulating the expected TDEM responses for a near-perfect conductor buried within a halfspace. Future work will be aimed at validating the augmented formulation for problem geometries of increasing complexity.

Keywords: TDEM, mineral exploration, numerical modeling

INTRODUCTION

Inductive source time-domain electromagnetic (TDEM) methods are frequently used to image ore-bearing mineralizations that present as thin, or plate-like. TDEM responses from these targets have historically been characterized with plate-modeling approaches (Hanneson and West, 1984; Walker and Lamontagne, 2006). Unfortunately, plate-modeling becomes decreasingly viable as geological complexity increases. 3D voxel-based approaches are not limited by geological complexity. However, the computational cost of 3D voxel-based algorithms becomes prohibitive when targets are sufficiently thin and/or conductive. The need to properly characterize inductive TDEM responses from thin, highly conductive targets (>1000 S/m) in geologically complex areas has promoted significant interest in developing improved numerical algorithms.

Progress has been made in the development of voxel-based algorithms for imaging thin and highly conductive structures. Weiss (2017) developed a finite element approach to solve the DC resistivity problem, wherein model parameters defining plate-like structures are defined on cell faces and model parameters defining wire-like structures are defined on cell edges. Hu et al (2022) adapted the original concept to develop a mimetic finite volume approach for well-casing applications in the frequency-domain. However, previous studies do not include TDEM problems and focus primarily on galvanic sources.

In this abstract, we augment the mimetic finite volume approach described in Haber (2014) to simulate inductive TDEM responses for highly conductive plate-like structures. We do this by augmenting the inner-product matrix obtained from Ohm's law to include contributions from volumetric currents that live within cells, surface currents that live on cell faces and line currents that live on cell edges. The formulation is implemented using the SimPEG (Cockett et al, 2015) framework. For now, our study will be limited to problem geometries that include volumetric and surface currents. Our formulation is validated for a large circular loop transmitter over a thin horizontal layer within a halfspace, where the electrical properties of the layer are defined as conductances which live on mesh faces. For a coincident loop airborne survey line, simulation on an OcTree mesh is used to demonstrate how the transient response changes as the conductance of buried plate-conductor increases.

MIMETIC FINITE VOLUME

The TDEM fields for a controlled electromagnetic source are obtained by solving Maxwell's equations. Ignoring electric displacement, the equations are:

$$\nabla \times \vec{e} + \frac{\partial \vec{b}}{\partial t} = -\vec{s}_m \tag{1a}$$
$$\nabla \times \vec{h} - \vec{j} = \vec{s}_e \tag{1b}$$
$$\vec{j} = \sigma \vec{e} \tag{1c}$$
$$\vec{h} = \mu^{-1} \vec{b} \tag{1d}$$

where $\vec{s}_e$ and $\vec{s}_m$ represent electric and magnetic source terms, respectively.

Applying the mimetic finite volume approach and using the weak form with natural boundary conditions, we obtain the following set of semi-discrete linear expressions (Haber, 2014):

$$\mathbf{Ce} + \frac{\partial \mathbf{b}}{\partial t} = -\mathbf{s_m} \tag{2a}$$
$$\mathbf{C^T M_f h} - \mathbf{M_e j} = \mathbf{s_j} \tag{2b}$$
$$\mathbf{M_e j} = \mathbf{M_{e\sigma} e} \tag{2c}$$
$$\mathbf{M_f h} = \mathbf{M_{f\frac{1}{\mu}} b} \tag{2d}$$

where $\mathbf{C}$ is the discrete curl operator, $\mathbf{M_e}$ and $\mathbf{M_f}$ are inner-product matrices for variables that live on edges and faces respectively, $\mathbf{M_{e\sigma}}$ is the inner-product matrix for electrical conductivities σ projected to edges, and $\mathbf{M_{f\frac{1}{\mu}}}$ is the inner-product matrix for inverse magnetic permeabilities μ^{-1} projected to faces.

Expressions 2a-d can be combined to obtain a second-order discrete expression for the electric fields $\mathbf{e}$ on mesh edges:

$$\mathbf{C^T M_{f\frac{1}{\mu}} Ce} + \mathbf{M_{e\sigma}} \frac{\partial \mathbf{e}}{\partial t} = -\mathbf{C^T M_{f\frac{1}{\mu}} s_m} - \frac{\partial \mathbf{s_e}}{\partial t} \tag{3}$$

Or a discrete expression for the magnetic flux densities $\mathbf{b}$ on mesh faces:

$$\mathbf{C M_{e\sigma}^{-1} C^T M_{f\frac{1}{\mu}} b} + \frac{\partial \mathbf{b}}{\partial t} = \mathbf{C M_{e\sigma}^{-1} s_e} - \frac{\partial \mathbf{s_m}}{\partial t} \tag{4}$$

Within SimPEG (Cockett et al, 2015), expressions 3 and 4 are discretized in time using backward Euler and solved at a finite set of time-steps.

VOLUME, FACE AND EDGE PROPERTIES

Here, we define a new parameterization for the Earth's electrical properties by decomposing the current density into volumetric currents that live within cells, surface currents that live on cell faces and line currents that live on cell edges. When taking the inner-product between a test function $\vec{u}$ and Ohm's law (Eq. 1c), we obtain:

$$\begin{aligned} \int_\Omega \vec{u} \cdot \vec{j} \, dv = & \sum_k^{nC} \int_{V_k} \vec{u} \cdot \sigma_k \vec{e} \, dv \\ & + \sum_k^{nF} \int_{A_k} \vec{u} \cdot \tau_k \vec{e} \, da \\ & + \sum_k^{nE} \int_{L_k} \vec{u} \cdot \lambda_k \vec{e} \, d\ell \end{aligned} \tag{5}$$

where σ_k defines the conductivity within cell k, τ_k defines the conductance for face k, and λ_k defines the conductivity integrated over the cross-sectional area of a wire element that lives on edge k. Figure 1 illustrates where the volume, face and edge properties live. Assuming cell faces and edges are infinitesimally thin, surface currents normal to surfaces and edge currents normal to edges are negligible. The discrete relationship between the current density and the electric field is given by:

$$\mathbf{M_e j} = \left[\mathbf{M_{e\sigma}} + \mathbf{M_{e\tau}} + \mathbf{M_{e\lambda}} \right] \mathbf{e} \tag{6}$$

where $\mathbf{M_{e\tau}}$ is the inner-product matrix for face conductivities projected to edges and $\mathbf{M_{e\lambda}}$ is the inner-product matrix for the electrical properties of the wire elements projected to edges. To account for face and edge currents, the augmented formulation replaces $\mathbf{M_\sigma}$ with $\mathbf{M_{e\sigma}} + \mathbf{M_{e\tau}} + \mathbf{M_{e\lambda}}$ in Eqs. 3 and 4.

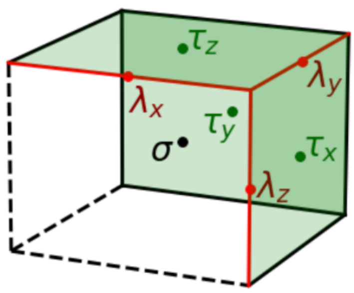

Figure 1: Discretization of volume conductivities (σ), face conductances (τ_x, τ_y, τ_z) and integrated conductivities on edges ($\lambda_x, \lambda_y, \lambda_z$).

1D Layered Earth Validation

Here, we validate the augmented finite volume formulation against a semi-analytic solution for a 1D layered Earth (Ward and Hohmann, 1988). We simulate the transient response at the center of a horizontal circular loop transmitter with a radius of 12 m located on the Earth's surface. The Earth is comprised of a thin horizontal layer within a 2.5e-3 S/m halfspace. The depth to the layer is 64 m. The layer is given a thickness of 0.1 m and a conductivity of 1e3 S/m (100 S conductance).

The augmented solutions to Eqs. 3 and 4 are solved on a cylindrically symmetric mesh and on an OcTree mesh, where the layer is defined by conductances that live on the appropriate mesh faces. Mesh discretization is determined by the diffusion distance of the host and the smoothness of the plate's surface currents. The cylindrically symmetric mesh has a minimum cell size of 2 m and a total of 36,250 m cells. The OcTree mesh has a cell size of 2 m near the source and 8 m near the layer, for a total of 29,464 mesh cells.

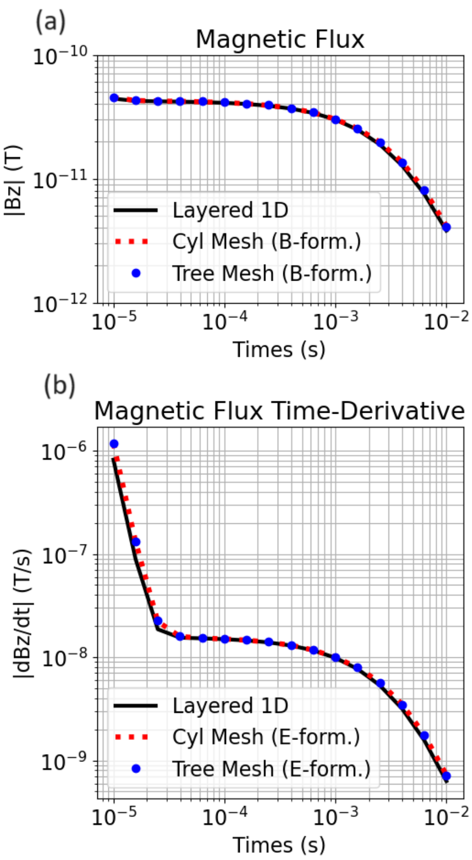

Figure 2: Validation for a horizontal layer within a halfspace (a) B-field. (b) dB/dt.

The vertical magnetic flux density and its time-derivative are illustrated in Figure 2. For both a cylindrically symmetric mesh and an OcTree mesh, Figure 2a shows that the B-formulation accurately simulates the magnetic flux density at the center of the loop for a reasonable number of mesh cells. For both a cylindrically symmetric mesh and an OcTree mesh, Figure 2b shows that the E-formulation accurately simulates the its time-derivative at the center of the loop for a reasonable number of mesh cells. Numerical accuracy remained consistent when the layer conductivity was increased.

Transient Response for a Highly Conductive Plate

As the conductance of a plate-like target increases, so does the decay constant characterizing its inductive response. For extremely high conductances, we expect the transient B-field response for a coincident loop system to remain static over the range of measured time channels. Additionally, we expect the transient dB/dt response to become insensitive to the target. Here, we demonstrate that the augmented finite volume formulation is capable of simulating the expected transient B-field and dB/dt responses for plate-like targets with moderate and extreme conductances.

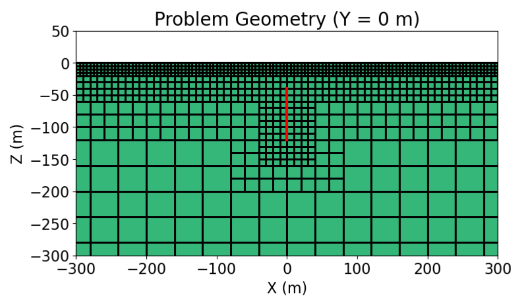

Figure 3: Vertical plate problem geometry.

The augmented forms of Eqs. 3 and 4 are used to simulate transient B-field and dB/dt data for a coincident loop airborne profile. The data are simulated on an OcTree mesh with a minimum cell size of 5 m and a total of 34,112 mesh cells. The conductivity model consists of a vertically oriented plate within a 1e-3 S/m halfspace. The plate is square, striking in the North-South direction, has a side length of 80 m, and its top is buried at a depth of 40 m. The electrical properties of the plate are defined as conductances that live on cell faces. Here, the data are simulated for a halfspace, and for plates with conductances of 1e2 S and 1e9 S.

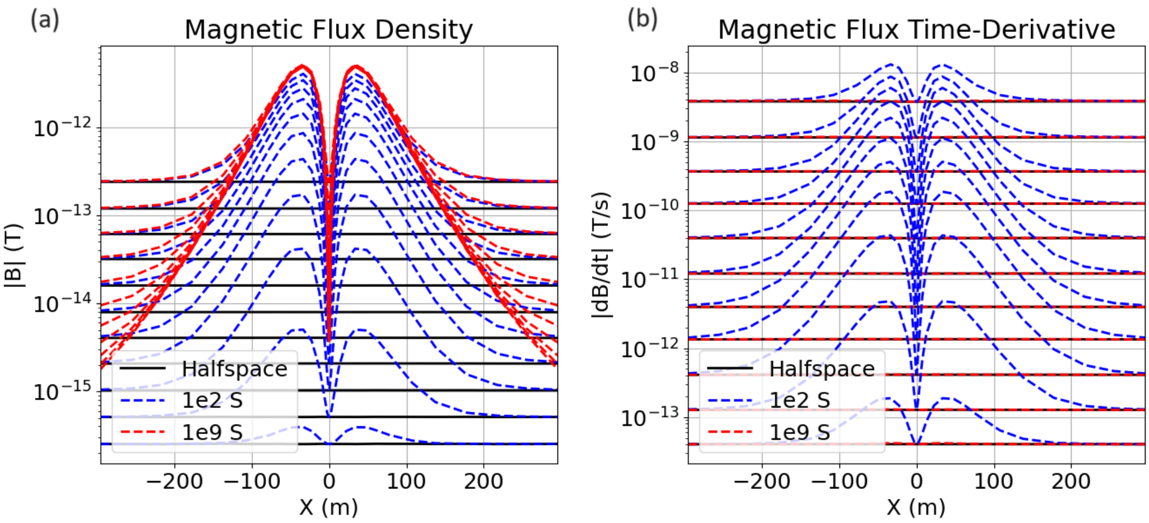

Figure 4: Airborne coincident loop data over a vertical plate. (a) B-field. (b) dB/dt.

The airborne profiles for the transient B-field and dB/dt responses are plotted in Figure 4. In the absence of the plate-like target, the transient B-field response decays proportional a $t^{-3/2}$ and the dB/dt response decays as $t^{-5/2}$. For a plate with moderate conductance (1e2 S), the time-constant is sufficiently small compared to the range of measured time-channels. As a result, the plate's B-field and dB/dt responses have decayed significantly by the latest time channel. For a nearly perfect conductor (1e9 S) however, we remain at the inductive limit over the range of measured time channels. As such, the transient B-field response from the target remains static, and exhibits no signature in the dB/dt response.

Conclusion

The need to properly characterize inductive responses from thin, highly conductive targets in geologically complex areas has promoted significant interest in developing improved numerical algorithms. Our work indicates that inductive TDEM responses from highly-conductive plate-like targets within an arbitrary host can be accurately simulated by defining plate-conductances on mesh faces. Furthermore, the augmented formulation is capable of simulating transient responses for near-perfect conductors. We showed that the required level of discretization near the plate does not depend on the plate's conductivity. Therefore we expect the formulation to remain computationally viable even for extremely conductive targets. Future work will be focused on validating the augmented formulation for problem geometries with increasing complexity.

References

Cockett R, Kang S, Heagy LJ, Pidlisecky A, Oldenburg DW (2015) Simpeg: An open source framework for simulation and gradient based parameter estimation in geophysical applications. Computers & Geosciences

Haber E (2014) Computational Methods in Geophysical Electromagnetics. Society for Industrial and Applied Mathematics, USA

Hanneson JE, West GF (1984) The horizontal loop electromagnetic response of a thin plate in a conductive earth; Part II, Computational results and examples. Geophysics 49(4):421–432, DOI 10.1190/1.1441677

Hu Y, Yang D, Li Y, Wang Z, Lu Y (2022) 3-d numerical study on controlled source electromagnetic monitoring of hydraulic fracturing fluid with the effect of steel-cased wells. IEEE transactions on geoscience and remote sensing 60:1–10

Walker P, Lamontagne Y (2006) Electromagnetic Interpretation In Complex Geological Environments. SEG International Exposition and Annual Meeting, vol All Days, pp SEG–2006–1288

Ward SH, Hohmann GW (1988) Electromagnetic theory for geophysical applications. Society of Exploration Geophysicists

Weiss CJ (2017) Finite-element analysis for model parameters distributed on a hierarchy of geometric simplices. Geophysics 82(4):E155–E167, DOI 10.1190/geo2017-0058.1